

# Fundamental Process of the Self-Organization of Waterway Network in Granular Material

農工大 工 G.P.ラジャセカール(G.P.RajaSekhar)  
農工大 工 佐野 理 (Osamu Sano)

*Department of Applied Physics, Tokyo University  
of Agriculture and Technology, Fuchu, Tokyo 183-0054*

## Abstract

The effect of the presence of a circular void of radius  $R_0$  in a porous media with permeability  $k$  on an otherwise undisturbed uniform flow  $U_\infty$  is investigated analytically. The entire flow field is determined by matching the solution of the Stokes equation inside the hole with that of the generalized Darcy's (Brinkman) equations in the porous region. Along the same lines, we have also estimated the flow field due to the deformed void whose shape is given by  $r = R_0(1 + \epsilon \cos m\theta)$ , where  $\epsilon \ll 1$  and  $m$  is an integer. The volume flow into the void region, and the velocity field in and around the void space, are compared with those for the void with complete circular boundary.

## I Introduction

Study of flow through porous media has drawn much attention due to its practical importance. Large number of applications are made in fields like geophysics, groundwater study, chemical engineering and macromolecular science. The present problem of our interest is a two-fold. First one is an application in groundwater studies and the second one is related to the generation of cavities and waterway network, or landslides due to seepage of rain into the ground.

For example, the application to groundwater studies meets an essential difficulty of determining the accurate velocity from the measured data of the groundwater velocity in a single borehole, because the introduction of the borehole into the soil changes the otherwise uniform flow field. Thus the theory to accurately estimate the flow field without a borehole is needed. The analytical treatment we have attempted helps us in finding the suitable application towards the measurement of the groundwater velocity using single boring method.

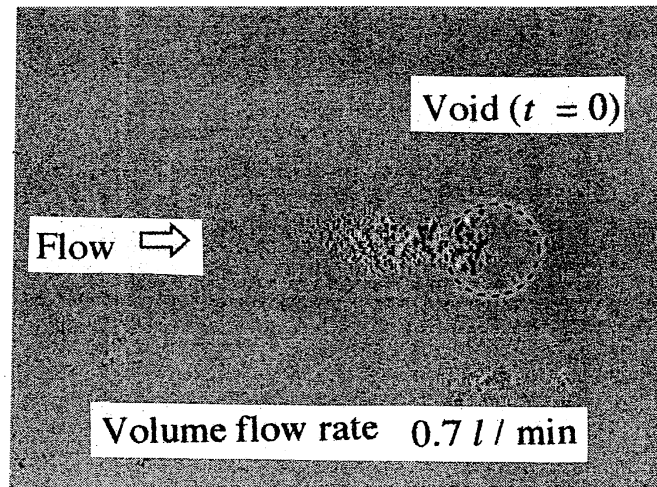


Fig.1 (a) Experimentally observed deformation of the void followed by the collapse.

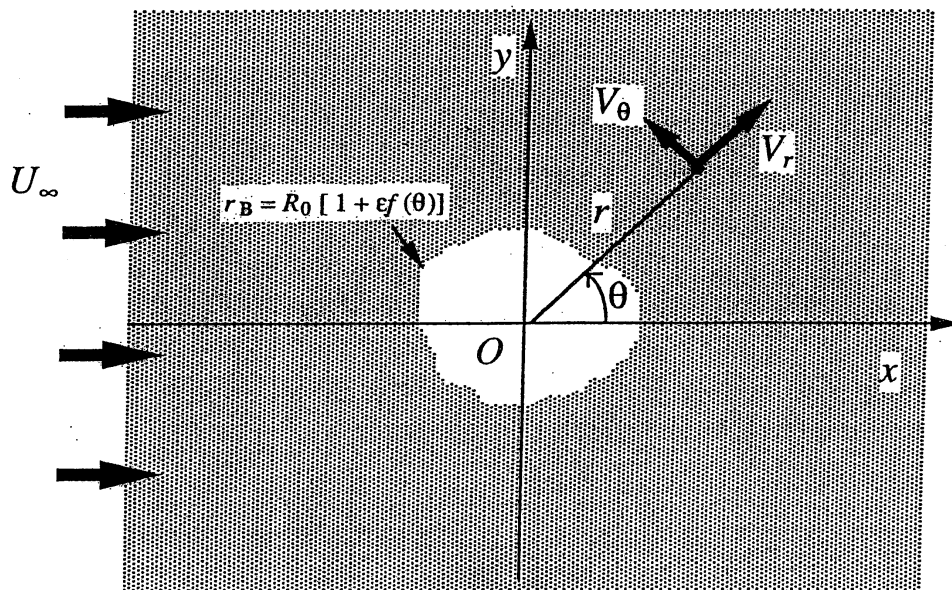


Fig.1 (b) Definition of the coordinate system.

Second one is the treatment of the situation when the void starts deforming due to the normal stress acting on the surface of the void. Because, our preliminary experiment on this shows that the particles on the upstream side start moving towards the downstream side through the void and that the void starts deforming slowly, which is followed by a collapse of the void (see Fig.1 (a)). The understanding of the latter phenomena, i.e., deformation of the void, is very important, because it is related to the generation of cavities and waterway network, or landslides due to seepage of rain into the ground.

## II Formulation

Let us consider an otherwise unbounded homogeneous porous medium in which there is a two-dimensional circular void space of radius  $R_0$ . The configuration of the coordinate system in Cartesian  $(x, y)$  form is such that  $x$ - axis is along the undisturbed uniform flow  $U_\infty$  at infinity. The corresponding polar coordinate system  $(r, \theta)$  is also shown in Fig.1 (b). On the basis of our previous studies (Sano,1983; RajaSekhar & Sano,2000), we assume that the flow in the porous region  $r \geq R_0$  is governed by the generalised Darcy's equation (Brinkman's equation), so that the velocity  $\mathbf{v}^e$  and pressure  $p^e$  satisfy the following equation:

$$\mu \nabla^2 \mathbf{v}^e = \nabla p^e + \frac{\mu}{k} \mathbf{v}^e, \quad (1)$$

$$\nabla \cdot \mathbf{v}^e = 0, \quad (2)$$

where  $k$  is the permeability of the porous medium and  $\mu$  is the viscosity. We use the superscript  $e$  and  $i$  to indicate that the flow is external to and internal to, respectively, the void region. The flow inside the void region  $r \leq R_0$  is governed by the Stokes equations given by

$$\mu \nabla^2 \mathbf{v}^i = \nabla p^i, \quad (3)$$

$$\nabla \cdot \mathbf{v}^i = 0. \quad (4)$$

The boundary conditions we employ are the continuity of the velocity components and the continuity of stress components on the surface of the void:

$$v_j^i = v_j^e, \quad (5)$$

$$t_{jk}^i = t_{jk}^e, \quad (6)$$

where  $j, k = x, y$  or  $r, \theta$  depending on the relevant coordinate system. We notice that in our preliminary work (1983, 2000), we obtained the flow past a cylindrical hole bored inside porous media using these boundary conditions, which agrees quite

well with the experimental results by Momii et al (1989).

### III Method of Solution

We first use the following transformation and non-dimensionalise the physical quantities:

$$(\tilde{\mathbf{x}}, \tilde{r}) = \frac{(\mathbf{x}, r)}{R_0}, \quad \tilde{\mathbf{v}} = \frac{\mathbf{v}}{U_\infty}, \quad \tilde{p} = p / \left( \mu \frac{U_\infty}{R_0} \right), \quad \zeta = \frac{r}{\sqrt{k}}, \quad \zeta_0 = \frac{R_0}{\sqrt{k}}. \quad (7)$$

Note that the parameter  $\zeta_0$  is a measure of the size of the void compared with the interstices between granular particles. Thus the governing equations in non-dimensional form become

$$(\tilde{\nabla}^2 - \zeta_0^2) \tilde{\mathbf{v}}^e = \tilde{\nabla} \tilde{p}^e, \quad (8)$$

$$\tilde{\nabla} \cdot \tilde{\mathbf{v}}^e = 0, \quad (9)$$

for the porous region and

$$\tilde{\nabla}^2 \tilde{\mathbf{v}}^i = \tilde{\nabla} \tilde{p}^i, \quad (10)$$

$$\tilde{\nabla} \cdot \tilde{\mathbf{v}}^i = 0, \quad (11)$$

for the region inside the void. Hereafter, however, we drop  $\tilde{\phantom{x}}$  for the dimensionless quantities for the sake of convenience.

In the porous region, where the velocity and pressure obey equations (8) and (9), the pressure is harmonic, so that we assume

$$p^e = -\zeta_0^2 r \cos \theta + \sum_{n=1}^{\infty} A_n r^{-n} \cos n\theta, \quad (12)$$

where  $A_n$  are arbitrary constants. In the above expressions symmetry of the flow field with respect to the flow direction and the shape of the void space, as well as the boundary condition at infinity, are considered. The velocity components of the flow in the porous region are assumed to be

$$v_r^e = \sum_{n=1}^{\infty} F_n(r) \cos n\theta, \quad (13)$$

$$v_\theta^e = \sum_{n=1}^{\infty} G_n(r) \sin n\theta, \quad (14)$$

where the forms of the functions  $F_n(r)$  and  $G_n(r)$  are determined so as to satisfy the eqs.(8) and (9). For the region inside the void, pressure is also harmonic and has

no singularity at the origin, so that we assume

$$p^i = \sum_{n=1}^{\infty} C_n r^n \cos n\theta, \quad (15)$$

and

$$v_r^i = \sum_{n=1}^{\infty} f_n(r) \cos n\theta, \quad (16)$$

$$v_\theta^i = \sum_{n=1}^{\infty} g_n(r) \sin n\theta, \quad (17)$$

for the velocity components, where the forms of the functions  $f_n(r)$  and  $g_n(r)$  are determined so that they satisfy the governing eqs. (10) and (11). Substitution of the expressions (12)-(17) for the corresponding governing equations (8) - (11), we obtain the general solutions for  $F_n, G_n, f_n, g_n$ , and hence the general solutions for the pressure and velocity components. They are

$$p^e = \left( -\zeta_0^2 r + \frac{A_1}{r} \right) \cos \theta + \sum_{n=2}^{\infty} \frac{A_n}{r^n} \cos n\theta, \quad (18)$$

$$v_r^e = \left( 1 + \frac{A_1}{\zeta_0^2 r^2} + \frac{B_1}{\zeta_0 r} K_1(\zeta_0 r) \right) \cos \theta + \sum_{n=2}^{\infty} \left( \frac{n A_n}{\zeta_0^2 r^{n+1}} + \frac{n B_n}{\zeta_0 r} K_n(\zeta_0 r) \right) \cos n\theta, \quad (19)$$

$$v_\theta^e = \left( -1 + \frac{A_1}{\zeta_0^2 r^2} - B_1 K_1'(\zeta_0 r) \right) \sin \theta + \sum_{n=2}^{\infty} \left( \frac{n A_n}{\zeta_0^2 r^{n+1}} - B_n K_n'(\zeta_0 r) \right) \sin n\theta, \quad (20)$$

for the porous region, and similarly

$$p^i = \sum_{n=1}^{\infty} C_n r^n \cos n\theta, \quad (21)$$

$$v_r^i = \sum_{n=1}^{\infty} \left( \frac{n C_n}{4(n+1)} r^{n+1} + D_n r^{n-1} \right) \cos n\theta, \quad (22)$$

$$v_\theta^i = \sum_{n=1}^{\infty} \left( -\frac{(n+2) C_n}{4(n+1)} r^{n+1} - D_n r^{n-1} \right) \sin n\theta, \quad (23)$$

for the region inside the void, where  $K_n(\zeta_0 r)$  are the Bessel functions of the second kind of order  $n$ , and  $A_n, B_n, C_n, D_n$  are the arbitrary constants to be determined using the boundary conditions.

Now, using the boundary conditions (5) - (6), and using the velocity components and pressure mentioned in (18) - (23), the complete flow field for the circular void is given by

$$p^e = \left( -\zeta_0^2 r + \frac{A_1}{r} \right) \cos \theta, \quad (24)$$

$$v_r^e = \left( 1 + \frac{A_1}{\zeta_0^2 r^2} + \frac{B_1}{\zeta_0 r} K_1(\zeta_0 r) \right) \cos \theta, \quad (25)$$

$$v_\theta^e = \left( -1 + \frac{A_1}{\zeta_0^2 r^2} - B_1 K_1'(\zeta_0 r) \right) \sin \theta, \quad (26)$$

for the porous region, and similarly

$$p^i = C_1 r \cos \theta, \quad (27)$$

$$v_r^i = \left( \frac{C_1}{8} r^2 + D_1 \right) \cos \theta, \quad (28)$$

$$v_\theta^i = \left( -\frac{3C_1}{8} r^2 - D_1 \right) \sin \theta, \quad (29)$$

where

$$A_1 = \frac{\zeta_0^2 [4\zeta_0 K_0 + (\zeta_0^2 + 8)K_1]}{\Delta_1}, \quad (30)$$

$$B_1 = -8 \frac{\zeta_0}{\Delta_1}, \quad (31)$$

$$C_1 = -8 \frac{\zeta_0^2 K_1}{\Delta_1}, \quad (32)$$

$$D_1 = \frac{8\zeta_0 K_0 + (3\zeta_0^2 + 16)K_1}{\Delta_1}, \quad (33)$$

$$\Delta_1 = 4\zeta_0 K_0 + (\zeta_0^2 + 16)K_1, \quad (34)$$

and where  $K_n \equiv K_n(\zeta_0)$  is the Bessel function of the second kind of order  $n$ .

#### IV Flow field due to the Circular Void

Figure 2(a) is the velocity distribution  $v_x (= -v_\theta(\theta = \pi/2))$  on the symmetry plane  $x = 0$ . The velocity profile is quadratic in the central region of the void, whose maximum speed increases with  $\zeta_0$ . In the limit of  $\zeta_0 \rightarrow \infty$ ,  $v_x$  reaches maximum speed of  $3U_\infty$  at the centre of the void. On the other hand  $v_x$  asymptotes to the undisturbed flow like

$$\frac{v_x}{U_\infty} = 1 - \frac{A_1}{\zeta_0^2 y^2} + \dots, \quad (35)$$

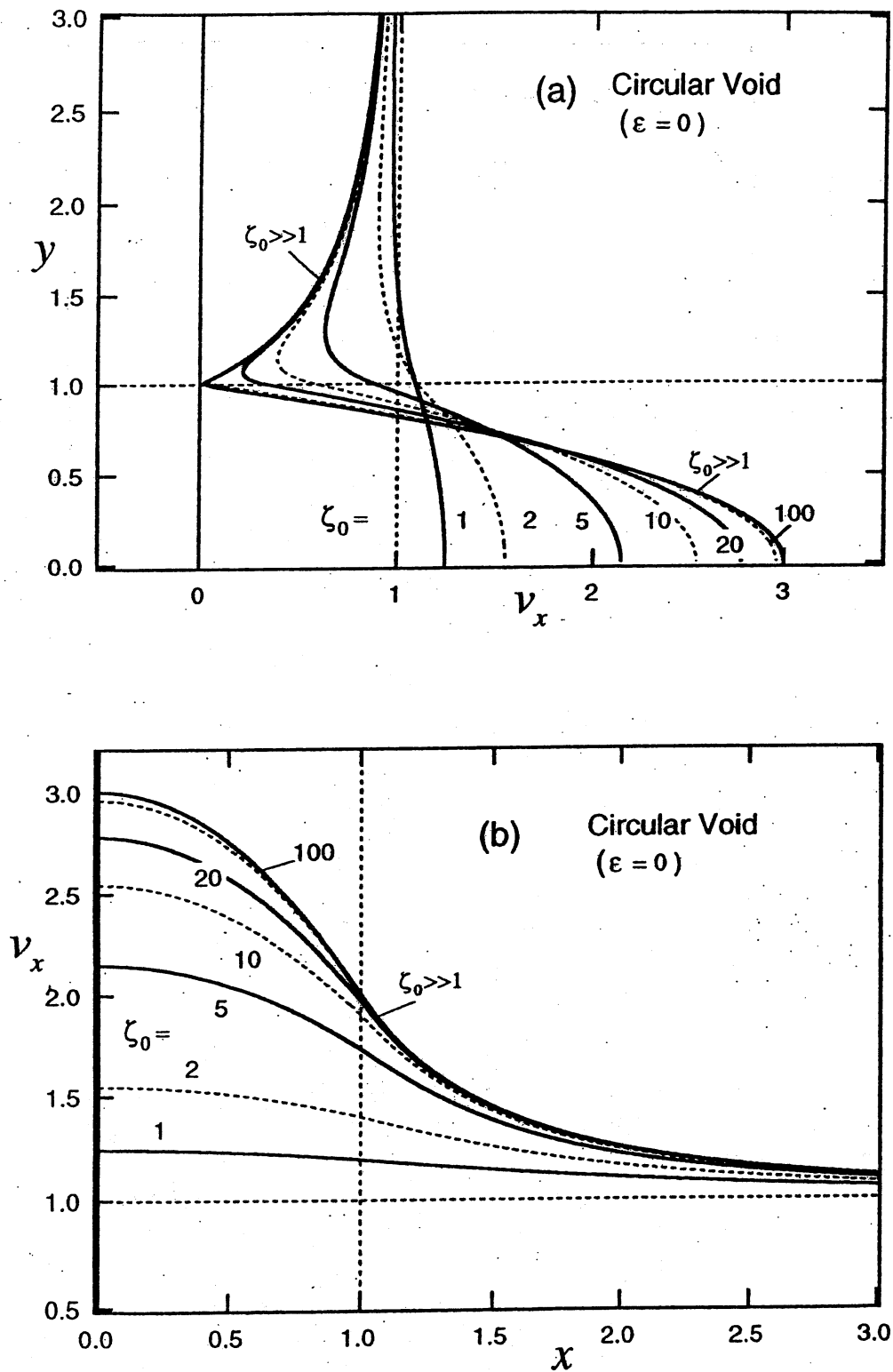


Fig.2 Velocity component  $v_x$  (a) on the  $x = 0$  plane and (b) on the  $y = 0$  plane, across the cylindrical hole of circular boundary ( $\epsilon = 0$ ).

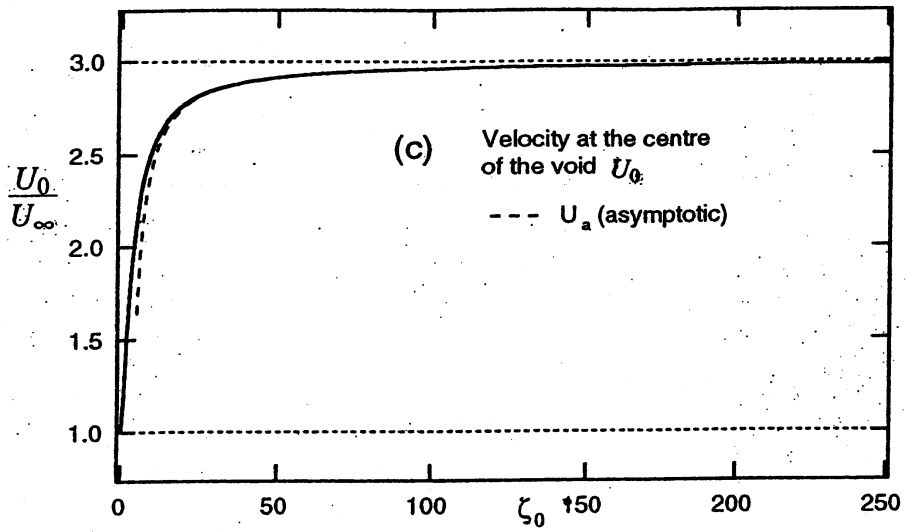


Fig.2 (c) Velocity at the centre of the void. Dashed line is the asymptotic behaviour given by eq.(35).

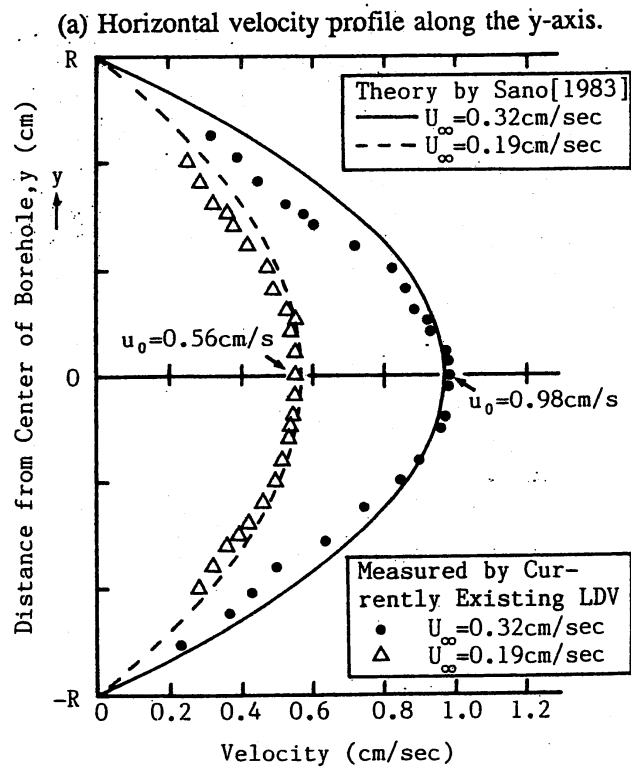


Fig.2 (d) Comparison of the velocity distribution  $v_x$  inside the borehole (Fig.2(a)) with experiment (Momii et al., 1989).

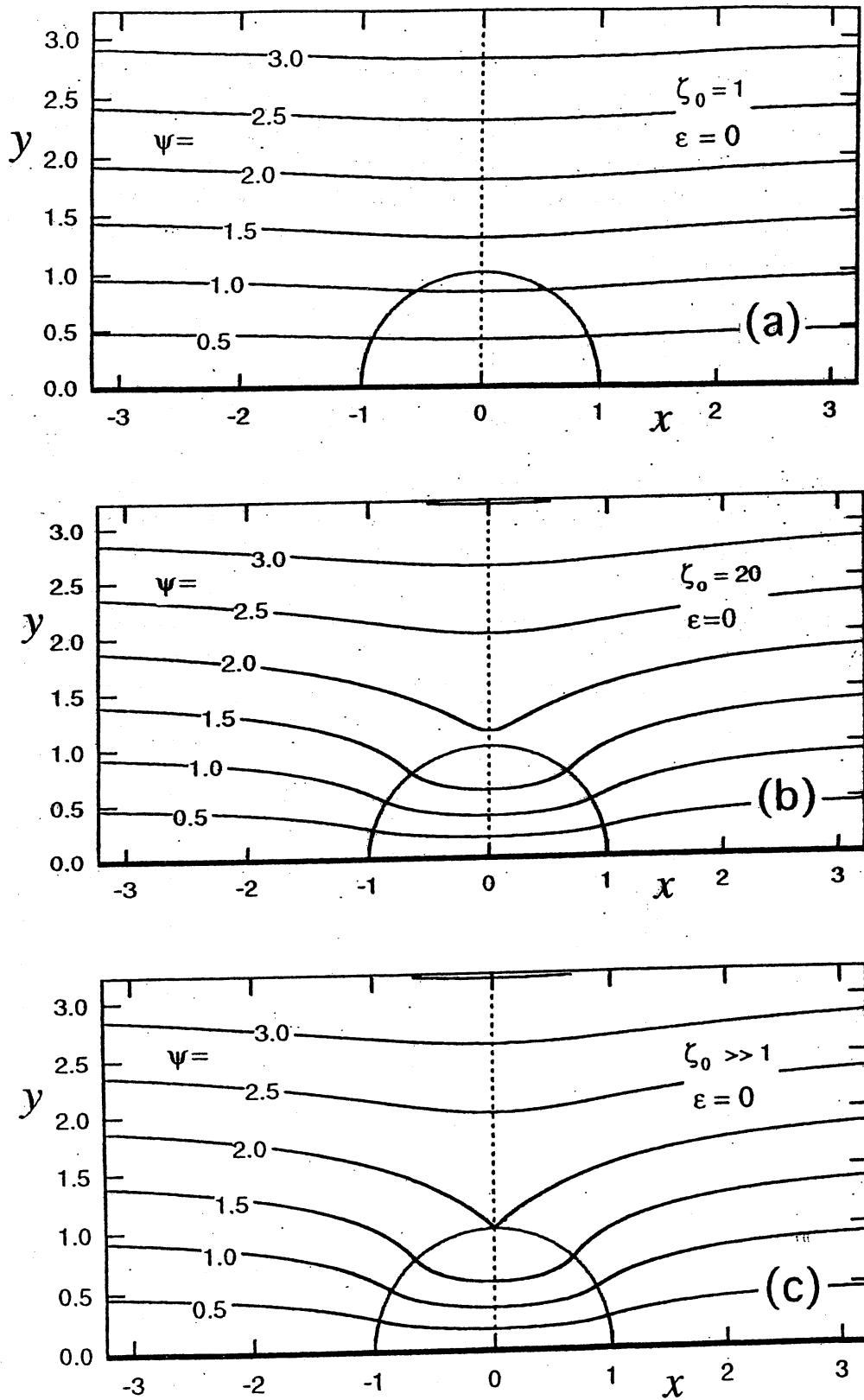


Fig.3 Streamlines around a void with different permeability (circular boundary); (a)  $\zeta_0 = 1$ , (b)  $\zeta_0 = 20$ , and (c)  $\zeta_0 \gg 1$ .

for  $\zeta_0 y \gg 1$ , where  $A_1$  is a function of  $\zeta_0$ . Near the boundary of the void, the magnitude of the velocity is reduced so as to satisfy the continuity of the fluid flow. Figure 2(b) shows the velocity distribution  $v_x (= v_r(\theta = 0))$  on the symmetry plane  $y = 0$ . Fluid motion is accelerated toward the centre of the void, and is decelerated to connect smoothly with undisturbed flow. Figure 2(c) shows the dependence of the velocity at the centre of the void  $U_0$  on  $\zeta_0$ , which approaches the maximum speed  $3U_\infty$  as  $\zeta_0$  tends to infinity :

$$\frac{U_0}{U_\infty} = 3 \left( 1 - \frac{4}{3\zeta_0} - \frac{14}{3\zeta_0^2} + \dots \right). \quad (36)$$

Agreement with experiment is remarkable (see Fig.2(d)).

Figures 3(a)-(c) are the streamlines around the void of complete circular boundary. The effect of the void increases with the increase of  $\zeta_0$ , which means the greater effect of a hole of given size on the granular material with the smaller permeability. For large permeability the flow is almost uniform-like (Fig.3(a)). However, for smaller permeability ( $\zeta_0 \gg 1$ ) the flow field is greatly perturbed (Fig.3(c)). A cusp is formed on the surface of the void, where the dividing streamline  $\psi = 2$  touches the void boundary. This means that the volume flux  $\psi_c$ , flowing into the cavity from upstream-side becomes twice, in comparison with  $\psi_\infty = wU_\infty$  that flows into the same region in the absence of the cavity, where  $2w$  is the lateral width of the cavity.

## V Deformed Void

For the particular situation where the circular void deforms slightly as  $r = 1 + \epsilon \cos m\theta$ , with  $\epsilon \ll 1$ , we expand the flow field and the boundary conditions in the power series of  $\epsilon$ , and obtain the solution by perturbation method up to the desired accuracy. As far as the first order of  $\epsilon$  is concerned, the boundary conditions (5) and (6) are given by

$$v_r^i = v_r^e, \quad v_\theta^i = v_\theta^e, \quad (37)$$

and

$$t_{rr}^i = t_{rr}^e, \quad t_{\theta r}^i = t_{\theta r}^e, \quad (38)$$

on the surface  $r = 1$ , where  $t_{rr}$  and  $t_{\theta r}$  are the normal and tangential stress components given by

$$t_{rr} = -p + 2\frac{\partial v_r}{\partial r}, \quad t_{\theta r} = \frac{1}{r}\frac{\partial v_r}{\partial \theta} + \frac{\partial v_\theta}{\partial r} - \frac{v_\theta}{r}.$$

The velocity components and pressure are determined by the above mentioned procedure. The flow in the porous region outside the void space is given by

$$p^e = \left(-\zeta_0^2 r + \frac{A_1}{r}\right) \cos \theta + \frac{A_{m+1}}{r^{m+1}} \cos(m+1)\theta, \quad (39)$$

$$v_r^e = \left(1 + \frac{A_1}{\zeta_0^2 r^2} + \frac{B_1}{\zeta_0 r} K_1(\zeta_0 r)\right) \cos \theta + \left(\frac{(m+1)A_{m+1}}{\zeta_0^2 r^{m+2}} + \frac{(m+1)B_{m+1}}{\zeta_0 r} K_{m+1}(\zeta_0 r)\right) \cos(m+1)\theta, \quad (40)$$

$$v_\theta^e = -\left(1 - \frac{A_1}{\zeta_0^2 r^2} + B_1 K_1'(\zeta_0 r)\right) \sin \theta + \left(\frac{(m+1)A_{m+1}}{\zeta_0^2 r^{m+2}} - B_{m+1} K_{m+1}'(\zeta_0 r)\right) \sin(m+1)\theta, \quad (41)$$

and the flow inside the void is given by

$$p^i = C_1 r \cos \theta + C_{m+1} r^{m+1} \cos(m+1)\theta, \quad (42)$$

$$v_r^i = \left(\frac{C_1}{8} r^2 + D_1\right) \cos \theta + \left(\frac{(m+1)}{4(m+2)} C_{m+1} r^{m+2} + D_{m+1} r^m\right) \cos(m+1)\theta, \quad (43)$$

$$v_\theta^i = -\left(\frac{3C_1}{8} r^2 + D_1\right) \sin \theta - \left(\frac{(m+3)}{4(m+2)} C_{m+1} r^{m+2} + D_{m+1} r^m\right) \sin(m+1)\theta, \quad (44)$$

where

$$A_n = \frac{2\epsilon\zeta_0^2}{\Delta_1\Delta_n} \left\{ K_n \left( \zeta_0^2 [4\zeta_0 K_0 + (\zeta_0^2 + 8)K_1] + 4n(n+1)[8\zeta_0 K_0 + (\zeta_0^2 + 16)K_1] \right) + 2\zeta_0(n+1)K_{n-1}[8\zeta_0 K_0 + (\zeta_0^2 + 16)K_1] \right\}, \quad (45)$$

$$B_n = -\frac{8\epsilon\zeta_0}{\Delta_1\Delta_n} \left\{ n(n+1)[8\zeta_0 K_0 + (\zeta_0^2 + 16)K_1] + \zeta_0^2(\zeta_0 K_0 + 2K_1) \right\}, \quad (46)$$

$$C_n = -\frac{8\epsilon\zeta_0^3}{\Delta_1\Delta_n} \left\{ n(n+1)\zeta_0 K_1 K_n - 2(n+1)(\zeta_0 K_0 + 2K_1)K_{n-1} \right\}, \quad (47)$$

$$D_n = \frac{2n\epsilon\zeta_0}{\Delta_1\Delta_n} \left\{ (n+1)\zeta_0^3 K_1 K_n + 2(n+1)[8\zeta_0 K_0 + (\zeta_0^2 + 16)K_1]K_{n-1} - 2\zeta_0^2(\zeta_0 K_0 + 2K_1)K_{n-1} \right\}, \quad (48)$$

$$\Delta_n = [\zeta_0^2 + 8n(n+1)]K_n + 2\zeta_0(n+1)K_{n-1} \quad (49)$$

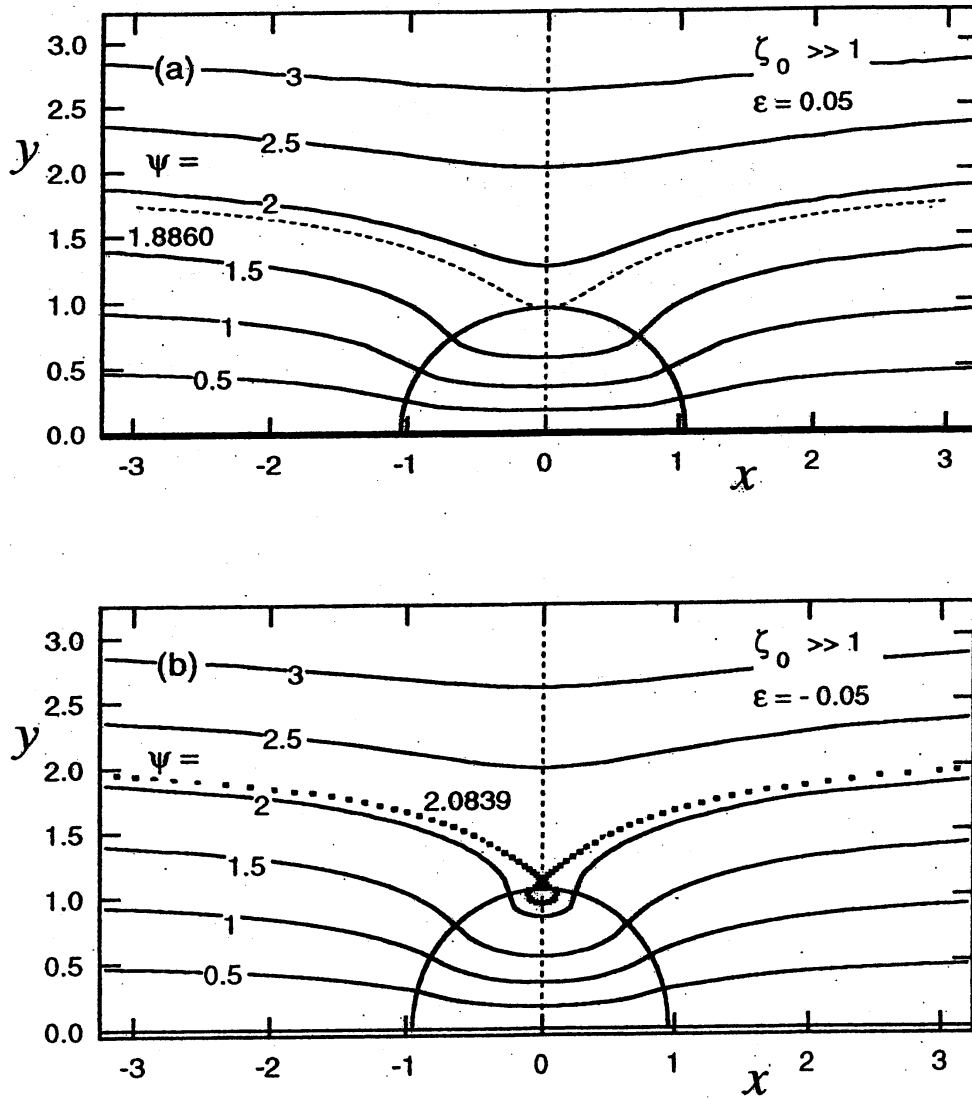


Fig.4 Streamlines around a deformed void  $r = 1 + \epsilon \cos 2\theta$  for  $\zeta_0 \gg 1$ ; (a)  $\epsilon = 0.05$  and (b)  $\epsilon = -0.05$ .

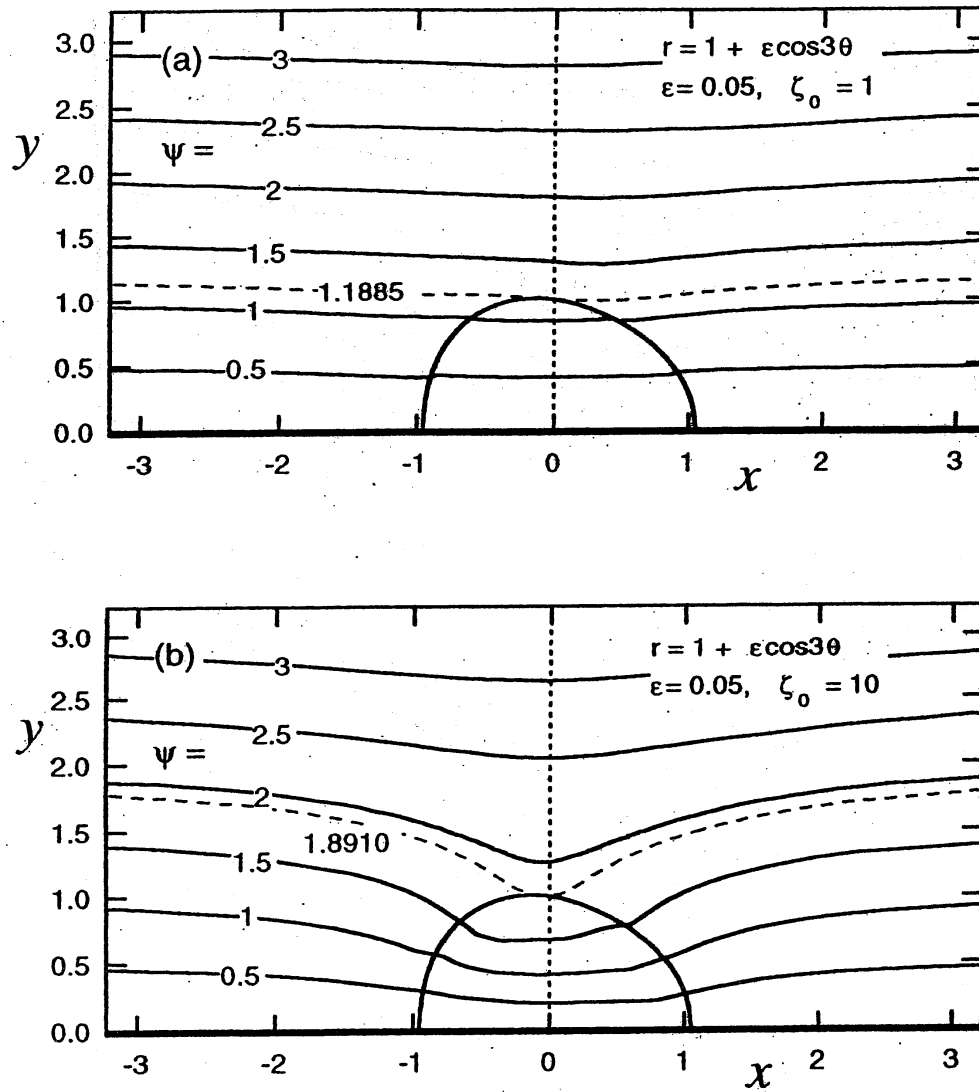


Fig.5 Streamlines around a deformed void  $r = 1 + \epsilon \cos 3\theta$  with  $\epsilon = 0.05$ ; (a)  $\zeta_0 = 1$ , (b)  $\zeta_0 = 10$ ,

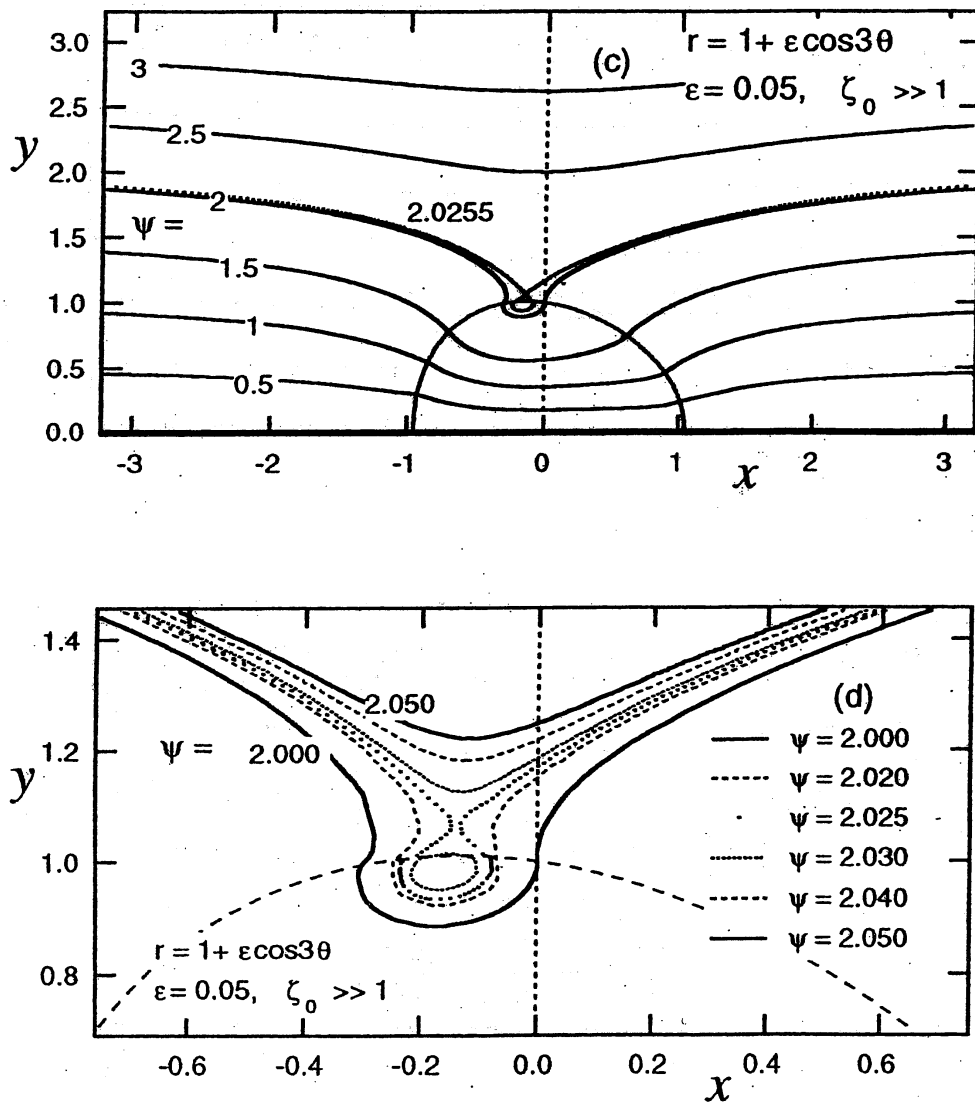


Fig.5 (continued)

(c)  $\zeta_0 \gg 1$  (d) a close-up view of (c) near the equator.

and  $A_1, B_1, C_1, D_1, \Delta_1$  are defined as in eqs. (30) - (34).

## VI Flow field due to the Deformed Void

### *Effect of a slight deformation with fore-and-aft symmetry*

Similar to the complete circular void case, the flow field is almost uniform-like for large permeability ( i.e.  $\zeta_0 = 1$ ), but is greatly disturbed for small permeability. Figures 4(a) and 4(b) are the streamlines for  $\epsilon = \pm 0.05$  for  $\zeta_0 \gg 1$ . For positive values of  $\epsilon$ , the void is elongated along the flow direction, while for negative values of  $\epsilon$  it is flattened. For  $\epsilon = 0.05$ , the dividing streamline  $\psi_c = 1.8860$  or  $\psi_c^* \equiv \psi_c/\psi_\infty = 1.9853$  touches the equator of the void. This means that there is a slight decrease in the volume flow rate compared with that for the complete circular void(Figs.6(a) and 6(b)). When  $\epsilon = -0.05$ , the flow is sensitive near the equatorial region, and a saddle-point-like behaviour is observed (Fig.4(b)). The cusp, which is observed on the dividing streamline  $\psi_c = 2.0839$  or  $\psi_c^* = 1.9847$ , is no longer on the surface of the void. The relative volume flow rate also decreases in comparison to the complete void case(Fig.6(b)).

### *Effect of a slight deformation with fore-and-aft asymmetry*

The case  $m = 3$  corresponds to the surface of the void  $r = 1 + \epsilon \cos 3\theta$ , which has a fore-and-aft asymmetry with respect to the  $y$ -axis. Dependence of the flow pattern on  $\zeta_0$  is shown in Figs.5(a)-5(c) for fixed value of  $\epsilon = 0.05$ . When the permeability is large (i.e.  $\zeta_0 = 1$ ), the flow is almost uniform-like(Fig.5(a)), but the volume flow rate into the void region is  $\psi_c = 1.1885$  or  $\psi_c^* = 1.1762$ , which means that the volume flow slightly decreases in comparison to the complete circular void case( $\psi_c = 1.1918$  in Fig.3(a) case). When the permeability is small (i.e.  $\zeta_0 = 10$ ), the flow pattern is greatly perturbed and the dividing streamline is  $\psi_c = 1.8910$  or  $\psi_c^* = 1.8715$ (Fig.5(b)). For very small permeability ( $\zeta_0 \gg 1$ ), the volume flow into the void region attains as large as  $\psi_c = 2.0255$  or  $\psi_c^* = 2.0046$  (Fig.5(c)). The close-up view of the streamlines near the surface of the void is shown in Fig.5(d), which shows a saddle-point-like behaviour, and the cusp is no longer on the surface of the void.

### *Effect of deformation on the volume flow rate*

Finally we summarize the dependence of volume flow rate into the void region  $\psi_c$  on  $\epsilon$  in Figs.6(a) and 6(b) for the most likely situation  $\zeta_0 \gg 1$ . For the symmetric void, the width of the hole across the otherwise uniform flow increases with decrease of  $\epsilon$ , which directly reflects the increase of volume flow(see Fig.6(a)). The relative

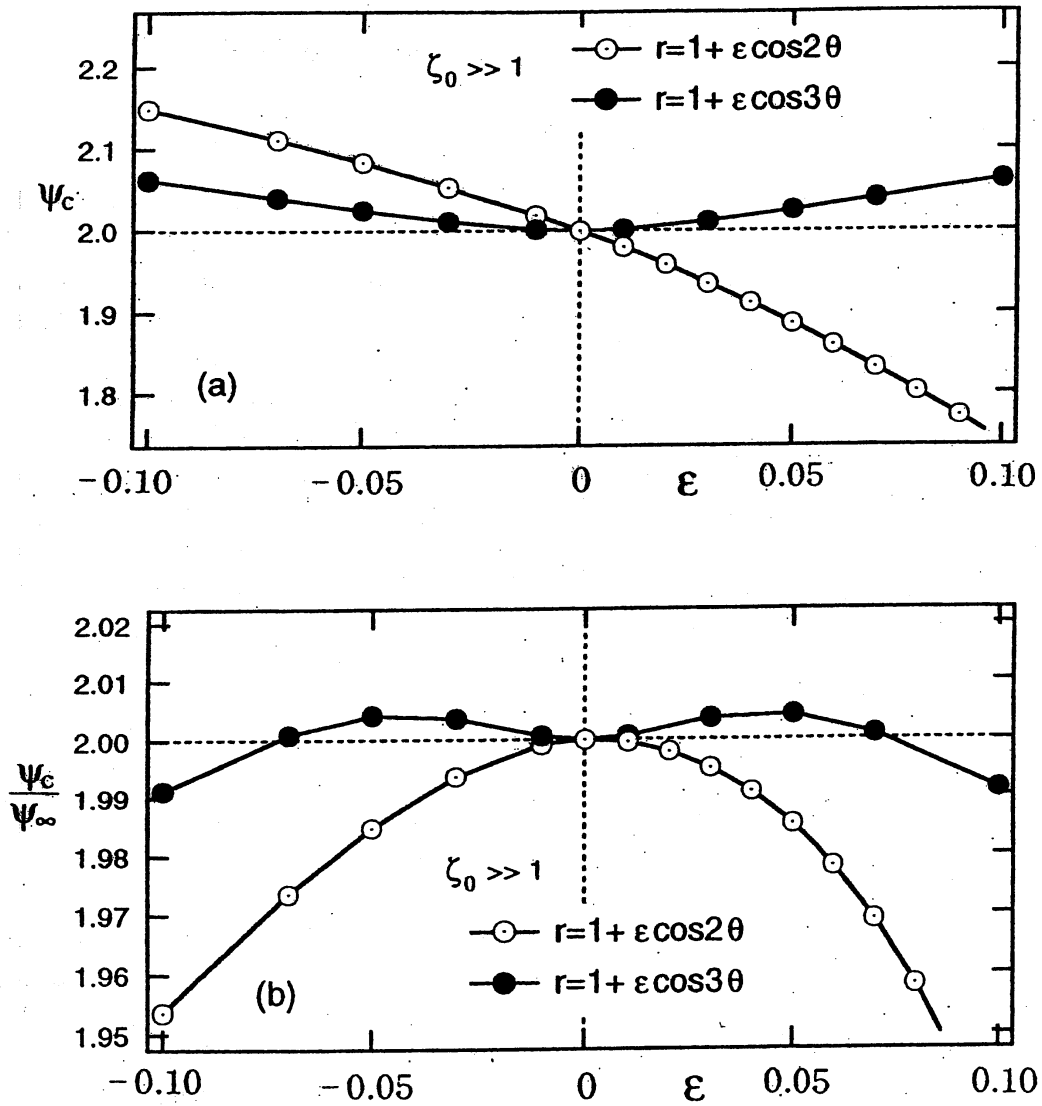


Fig.6 (a) Dependence of the volume flow rate  $\psi_c$  into the void region on  $\epsilon$  for  $\zeta_0 \gg 1$ . (b) Volume flow rate  $\psi_c^*$  normalized by the flow passing through the same region by the undisturbed uniform flow.

volume flow  $\psi_c^*$ , however, decreases as  $\epsilon$  decreases (see Fig.6(b)). Note that both  $\psi_c$  and  $\psi_c^*$  decrease as  $\epsilon$  increases, so that the relative volume flow rate of the void with fore-and-aft symmetry attains its maximum value for the circular void. On the other hand, in the case of asymmetric void discussed here, the volume flow rate  $\psi_c^*$  seems to have its maximum value at  $\epsilon \approx \pm 0.05$ .

By assuming that the granular material is collapsed for negative normal stress whose magnitude exceeds a certain threshold value, we can reproduce the deformation of the upstream-side of the void, which will be shown in our succeeding paper.

**Acknowledgement** This work is partially supported by the Grant-in-Aid for Scientific Research from the Ministry of Education, Science and Culture, Japan. One of the author GPR acknowledges Japan Society for the Promotion of Science for the financial support.

## References

- 1) Brinkman, H.C. (1947) A calculation of the viscous force exerted by a flowing fluid on a dense swarm of particles, *Appl. Sci. Res.* A1, 27-33.
- 2) Childress, S. (1972) Viscous flow past a random array of spheres, *J. Chem. Phys.* 56, 2527-2539.
- 3) Debye, P. and Bueche, A.M. (1948) Intrinsic viscosity, diffusion and sedimentation rate of polymers in solution, *J. Chem. Phys.* 16(6), 573-579.
- 4) Momii, K., Jinno, K., Ueda, T., Motomura, H., Hirano, F. and Honda, T. (1989) Experimental study on groundwater flow in a borehole, *J. Groundwater Hydrol.*, 31, 13-18.
- 5) RajaSekhar, G.P. and Sano, O. (2000) Viscous flow past a circular/spherical void in porous media — an application to measurement of the velocity of groundwater by single boring method, *J. Phys. Soc. Jpn.* 69, 2479 - 2484.
- 6) RajaSekhar, G.P. and Sano, O. (1999) Deformation of Void space in granular material due to induced flow, Proceedings of ISTAM, REC Warangal, India.
- 7) Sano, O. (1983) Viscous flow past a cylindrical hole bored inside porous media — with Application to Measurement of the Velocity of Subterranean Water by the Single Boring Method, *Nagare* 2, 252-259 (in Japanese).
- 8) Tam, C.K.W. (1969) The drag on a cloud of spherical particles in low Reynolds number flow, *J. Fluid Mech.* 38, 537-546.
- 9) Yano, H. and Kieda, A. (1991) The fundamental solution of Brinkman's equation in two dimensions, *Fluid Dyn. Res.* 7, 109-118.